

UDC 541.6:541.49:546.56:546.72

**NOVEL REPAGLINIDE COMPLEXES WITH MANGANESE(II), IRON(III), COPPER(II) AND ZINC(II): SPECTROSCOPIC, DFT CHARACTERIZATION AND ELECTROCHEMICAL BEHAVIOUR**

**S. Sadaoui-Kacel<sup>1,2</sup>, S. Zaater<sup>3</sup>, N. Bensouilah<sup>4</sup>, S. Djebbar<sup>1</sup>**

<sup>1</sup>*Laboratoire d'Hydrométallurgie et Chimie Inorganique Moléculaire, Faculté de Chimie, Université de Houari Boumediene Sciences et Technologie, Alger, Algérie*  
E-mail: safia.djebbar@netcourrier.com

<sup>2</sup>*Département de Chimie, Faculté des Sciences, Université de M'hamed Bougara, Boumerdès, Algérie*

<sup>3</sup>*Laboratoire de Physico-Chimie théorique et Chimie Informatique, Faculté de Chimie, Université de Houari Boumediene Sciences et Technologie, Alger, Algérie*

<sup>4</sup>*Laboratoire de Chimie Appliquée, Université 8 Mai 1945, Guelma, Algérie*

Received August, 12, 2015

Revised — May, 7, 2016

Novel transition metal complexes with the repaglinide ligand [2-ethoxy-4-[N-[1-(2-piperidinophenyl)-3-methyl-1-butyl] aminocarbonylmethyl]benzoic acid] (HL) are prepared from chloride salts of manganese(II), iron(III), copper(II), and zinc(II) ions in water-alcoholic media. The mononuclear and non-electrolyte  $[M(L)_2(H_2O)_2] \cdot nH_2O$  ( $M = Mn^{2+}$ ,  $n = 2$ ,  $M = Cu^{2+}$ ,  $n = 5$  and  $M = Zn^{2+}$ ,  $n = 1$ ) and  $[M(L)_2(H_2O)(OH)] \cdot H_2O$  ( $M = Fe^{3+}$ ) complexes are obtained with the metal:ligand ratio of 1:2 and the L-deprotonated form of repaglinide. They are characterized using the elemental and molar conductance. The infrared,  $^1H$  and  $^{13}C$  NMR spectra show the coordination mode of the metal ions to the repaglinide ligand. Magnetic susceptibility measurements and electronic spectra confirm the octahedral geometry around the metal center. The experimental values of FT-IR,  $^1H$  NMR, and electronic spectra are compared with theoretical data obtained by the density functional theory (DFT) using the B3LYP method with the LANL2DZ basis set. Analytical and spectral results suggest that the HL ligand is coordinated to the metal ions via two oxygen atoms of the ethoxy and carboxyl groups. The structural parameters of the optimized geometries of the ligand and the studied complexes are evaluated by theoretical calculations. The order of complexation energies for the obtained structures is as follows:



The redox behavior of repaglinide and metal complexes are studied by cyclic voltammetry revealing irreversible redox processes. The presence of repaglinide in the complexes shifts the reduction potentials of the metal ions towards more negative values.

DOI: 10.15372/JSC20160805

**Keywords:** metal complexes, repaglinide ligand, synthesis, DFT, electrochemical behavior.

## INTRODUCTION

For more than a decade, considerable attention has been paid to the chemistry of transition metal complexes containing nitrogen, oxygen, and other donors [1—5]. The chemical properties of compounds containing aromatic carboxyls have been extensively investigated because of their strong ten-

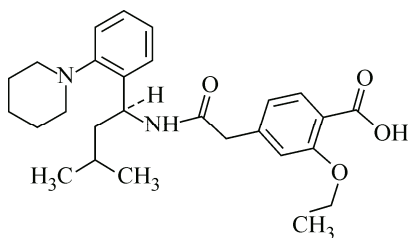


Fig. 1. Repaglinide ligand (HL)

tendency to chelate transition metals. Manganese, iron, copper, and zinc are essential trace elements responsible for the functioning of many cellular enzymes and proteins [6]. Repaglinide 2-ethoxy-4-[N-[1-(2piperidinophenyl)-3-methyl-1-butyl]aminocarbonylmethyl] benzoic acid (HL) (Fig. 1) is an antidiabetic agent from the class of glinides, used for the treatment of patients with type 2 diabetes mellitus [7]. In this work, we report the synthesis and characterization by analytical and spectral methods of novel repaglinide complexes with manganese(II), iron(III), copper(II), and zinc(II) and the study of the effect of repaglinide presence around the metal center on the stability of the complexes as well as its effect on the potential redox of the metal ion. DFT calculations are used to evaluate the structural parameters of the optimized geometries of the ligand and the studied complexes and confirm their stability by calculating complexation energies. The electrochemical properties of the ligand and its complexes are investigated in a DMSO solution containing 0.1 M tetrabutylammoniumhexafluorophosphate ( $n\text{Bu}_4\text{NPF}_6$ ) as supporting electrolyte by cyclic voltammetry.

## EXPERIMENTAL

**Reagents.** All chemicals were purchased from commercial sources (Sigma-Aldrich Co., Fluka Co.) and used as received without further purification.

**Synthesis of metal complexes.**  $[\text{Mn}(\text{L})_2(\text{H}_2\text{O})_2] \cdot 2\text{H}_2\text{O}$ . An aqueous solution of  $\text{MnCl}_2 \cdot 4\text{H}_2\text{O}$  (1 mmol) in bidistilled water (5 ml) was added dropwise to a solution of the HL ligand (2 mmol) in absolute ethanol (10 ml) in a 1:2 metal-to-ligand molar ratio. The pH was adjusted to 9 using sodium hydroxide (0.1 M). The resulting mixture was stirred for 2 h. One day later, the colored solid formed was filtered, washed with ethanol and distilled water, dried at 50 °C, and finally stored in a vacuum desiccator.

$[\text{Fe}(\text{L})_2(\text{H}_2\text{O})(\text{OH})] \cdot \text{H}_2\text{O}$ . A solution of  $\text{FeCl}_3 \cdot 6\text{H}_2\text{O}$  (1 mmol) in bidistilled water (5 ml) was added dropwise to a solution of the HL ligand (2 mmol) in absolute ethanol (10 ml) in a 1:2 metal-to-ligand molar ratio. The pH was adjusted to 4 using sodium hydroxide (0.1 M). The resulting mixture was stirred for 3 h. One day later, the colored solid formed was filtered, washed with ethanol, and distilled water, dried at 50 °C, and finally stored in a vacuum desiccator.

$[\text{Cu}(\text{L})_2(\text{H}_2\text{O})_2] \cdot 5\text{H}_2\text{O}$ . The copper (II) complex was synthesized by reacting 5 ml of an aqueous solution of  $\text{CuCl}_2 \cdot 2\text{H}_2\text{O}$  (1 mmol) with 10 ml of an ethanolic solution of the HL ligand (2 mmol) in a 1:2 metal-to-ligand molar ratio. The pH was adjusted to 7 using sodium hydroxide (0.1 M). The resulting mixture was stirred for 2 h. One day later, the colored solid formed was filtered, washed with ethanol and distilled water, dried at 50 °C. and finally stored in a vacuum desiccator.

$[\text{Zn}(\text{L})_2(\text{H}_2\text{O})_2] \cdot \text{H}_2\text{O}$ . A solution of  $\text{ZnCl}_2$  (1 mmol) in bidistilled water (5 ml) was added dropwise to a solution of the HL ligand (2 mmol) in absolute ethanol (10 ml) in a 1:2 metal-to-ligand molar ratio. The pH was adjusted to 8 using sodium hydroxide (0.1 M). The resulting mixture was stirred for 3 h. One day later, the colored solid formed was filtered, washed with ethanol and distiller water, dried at 50 °C, and finally stored in a vacuum desiccator.

**Physicochemical measurements.** Elemental analyses were performed with a Microanalyser Flash EA1112 CHNS/O apparatus at the "Centre Régional de Mesures Physiques" at the University of Rennes1, France. Manganese, iron, copper, and zinc were determined using a Solaar Thermo Elemental atomic absorption spectrophotometer. Molar conductance values of the complexes in DMSO were measured using a JENWAY-4520 conductometer at 25 °C; the solution concentration was  $10^{-3} \cdot \text{mol} \cdot \text{L}^{-1}$ . Melting points were measured with a BUCHI B-545 capillary melting point apparatus. IR spectra (4000—400  $\text{cm}^{-1}$ ) for KBr disks were recorded on a Perkin Elmer FT-IR spectrometer.

The  $^1\text{H}$  and  $^{13}\text{C}$  NMR spectra in a DMSO- $d_6$  solvent were recorded in a Bruker Avance DPX 400 and 100 MHz spectrometer. Chemical shifts are reported in parts per million downfield from tetramethylsilane as the internal reference. The electronic spectra were recorded in DMSO on a Jasco V-530

spectrophotometer in the range 190—900 nm. The magnetic measurements were carried out using a SQUID magnetometer in a 200—300 K range with an applied field of 10000 G. The electrochemical measurements were performed on an EDAQ Model EA161 apparatus Program EChem Version: 2.0.9. The cyclic voltammograms were measured at 20 °C under a nitrogen atmosphere using platinum electrodes, SCE as a reference electrode, and tetrabutylammonium hexafluorophosphate ( $n\text{Bu}_4\text{NPF}_6$ , 0.1 M) as supporting electrolyte.

**Molecular modeling.** The geometry of the synthesized complexes in gas was optimized with density functional theory (DFT) using Becke's three parameter hybrid method and the Lee—Yang—Parr correlation functional (B3LYP) [8] combined with the LANL2DZ basis set [9] using the Gaussian 03 program package [10]. The synthesized complexes were characterized as minima (no imaginary frequency) in their potential energy surface through the harmonic frequency analysis [11].

## RESULTS AND DISCUSSION

**Physical measurements.** The elemental analysis data of the complexes, given in Table 1, are consistent with the calculated results from the empirical formulae of each complex. The results of molar conductivity measurements suggest that all the synthesized complexes are non-electrolytes [12, 13]. The complexes are colored solids, insoluble in water, partly soluble in ethanol and methanol and soluble in DMSO and DMF.

**Infrared spectra.** The infrared spectra of repaglinide and its metal complexes were recorded in the range from 400 to 4000  $\text{cm}^{-1}$ . The IR spectra of metal complexes are compared with that of the free ligand in order to determine the coordination sites that may be involved in chelation. The infrared spectra of the ligand shows peaks at 3307  $\text{cm}^{-1}$  (NH stretching), 2947  $\text{cm}^{-1}$  (CH stretching), and 1728  $\text{cm}^{-1}$  (C=O stretching). In the infrared spectra of the complexes, bands assigned to NH stretching, CH stretching, and C=O stretching were identified at 3298—3308, 2936—2942, and 1679—1728  $\text{cm}^{-1}$ , respectively. The band at 1634  $\text{cm}^{-1}$  assigned to the  $\bar{\nu}(\text{C=O})$  vibration of the COOH carboxylic group is present in the ligand and disappears in the complexes, which means the involvement of the carboxylic group in the chelation with the metal ion. The asymmetric stretching vibration of the carboxylate group  $\bar{\nu}_{\text{as}}(\text{COO})^-$ , which appears at 1540, 1568, 1540, and 1548  $\text{cm}^{-1}$  for manganese (II), iron(III), copper(II), and zinc(II) complexes, respectively, are absent in the spectral data of the repaglinide ligand [16]. The broad bands in the range of 3423—3459  $\text{cm}^{-1}$  are attributed to the presence of hydrated water molecules and the bands observed at 842—815  $\text{cm}^{-1}$  are assigned to coordinated water molecules, which are confirmed by thermal analysis data. The vibrational assignments were carried out also with the support of DFT calculations using the B3LYP method with the LANL2DZ basis set. The experimental and theoretical FT-IR spectra of the manganese(II) complex are given in Fig. 2. The vibrational assignments are: 1598, 1599, 1596, and 1599  $\text{cm}^{-1}$  respectively, are in very good agreement with the experimental values of the asymmetric stretching vibration of the carboxylate group

Table 1

*Analytical data and some physical properties of the metal complexes*

Complexes	Exp. (Calc.), %				Melting point, °C	Yield, %	$\Lambda_{\text{DMSO}}$ , $\Omega^{-1} \cdot \text{cm}^2 \cdot \text{mol}^{-1}$
	C	H	N	M			
[Mn(L) <sub>2</sub> (H <sub>2</sub> O) <sub>2</sub> ]·2H <sub>2</sub> O	62.55 (62.90)	6.83 (7.57)	5.39 (5.43)	5.61 (5.33)	143	82	12.22
[Fe(L) <sub>2</sub> (H <sub>2</sub> O)(OH)]·H <sub>2</sub> O	64.56 (64.03)	7.56 (7.41)	5.61 (5.53)	5.72 (5.51)	131	68	7.50
[Cu(L) <sub>2</sub> (H <sub>2</sub> O) <sub>2</sub> ]·5H <sub>2</sub> O	59.23 (59.41)	7.01 (7.68)	5.20 (5.12)	5.94 (5.81)	140	57	6.82
[Zn(L) <sub>2</sub> (H <sub>2</sub> O) <sub>2</sub> ]·H <sub>2</sub> O	63.29 (64.50)	7.16 (7.36)	5.49 (5.57)	6.10 (6.39)	205	74	17.20

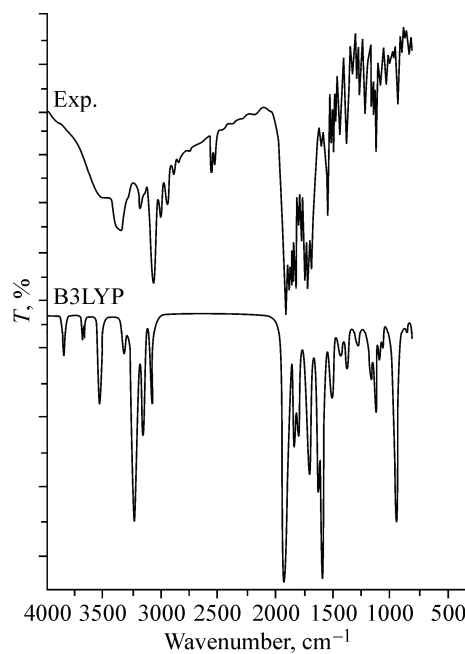


Fig. 2. IR (experimental and DFT) spectra in the 400—4000 cm<sup>-1</sup> region for the manganese(II) complex

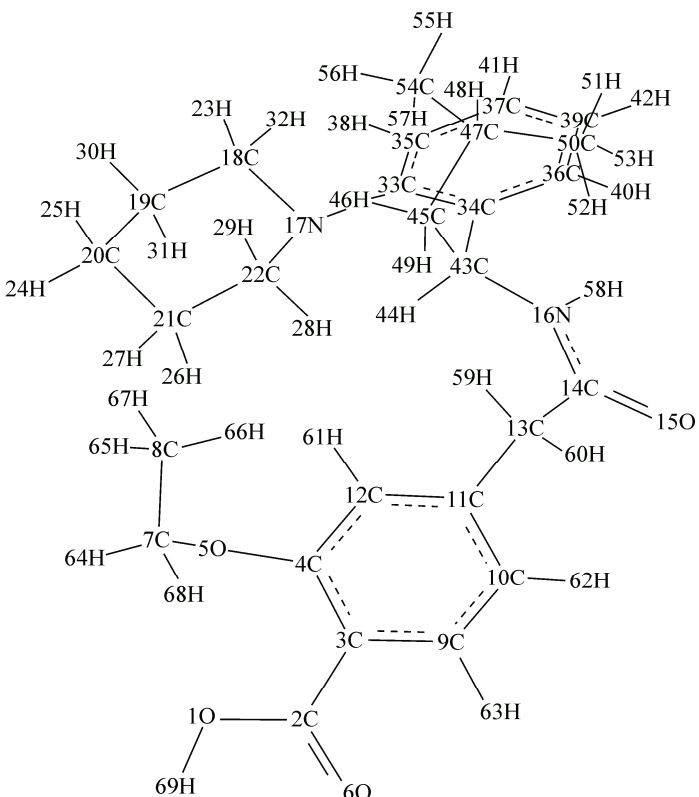


Fig. 3. Structure of the repaglinide ligand with numbering of hydrogen and carbon atoms

$\bar{v}_{as}$  (COO)<sup>-</sup>. The shift of the (C—O) band towards a higher frequency region in the complexes indicates its involvement in coordination with the metal ion. Its calculated counterpart is between 1201 to 1248 cm<sup>-1</sup> for the metal complexes. The assignment of the proposed coordination sites is further supported by the appearance of a band at 539—560 cm<sup>-1</sup> suggesting the  $\bar{v}$ (M—O) bond.

<sup>1</sup>H and <sup>13</sup>C NMR spectra. In the <sup>1</sup>H NMR spectrum of the zinc(II) complex, the integrated intensities of each signal were found to agree with the number of different types of protons present in the complex (Fig. 3). The <sup>1</sup>H NMR spectrum of HL shows a signal due to the presence of the OH proton of the carboxylic group at 12.37 ppm in the free HL ligand [17]. This signal is absent in the <sup>1</sup>H NMR spectrum of the zinc(II) complex suggesting its coordination to the metal which deprotonates during complexation.

The theoretical <sup>1</sup>H and <sup>13</sup>C NMR chemical shifts are evaluated also by DFT calculations. They are in reasonable agreement with those found experimentally. <sup>1</sup>H and <sup>13</sup>C NMR data confirm the coordination mode of repaglinide as reported previously in the IR study. The measured chemical shifts of all hydrogen and carbon atoms for the spectra of the Zn(II) complex are listed in Table 2.

Electronic spectra and magnetic moments. The electronic absorption spectra of the synthesized metal complexes were recorded in DMSO in the range 200—1000 nm, showing two bands that are due to intraligand transitions ( $n \rightarrow \pi^*$  and  $\pi \rightarrow \pi^*$ ) [18], at the range 26.100—34.843 cm<sup>-1</sup>.

The manganese complex in the DMSO solution shows a band at 23148 cm<sup>-1</sup> due to the metal-ligand charge transfer transition. The magnetic moment of this complex is  $\mu_{eff} = 4.96 \mu_B$ , which indicates the presence of the Mn(II) complex in the octahedral structure [19, 20]. The electronic spectrum of the iron complex displays two bands at 20366 and 13736 cm<sup>-1</sup>, which may be assigned to the  $^6A_{1g} \rightarrow T_{2g}$  and  $^6A_{1g} \rightarrow ^5T_{1g}$  transitions, indicating the octahedral geometry around the Fe(III) ion [21]. The calculated  $\bar{v}_2 / \bar{v}_1$  ratio is 1.48, suggesting an octahedral environment around the Fe(III) ion. The calculated crystal field parameters of this complex are  $10Dq = 13736 \text{ cm}^{-1}$  and  $B = 214 \text{ cm}^{-1}$ . The

Table 2

<sup>1</sup>H and <sup>13</sup>C NMR data of the zinc(II) complex

No. of hydrogen atoms	<sup>1</sup> H chemical shift δ, ppm	No. of hydrogen atoms	<sup>1</sup> H chemical shift δ, ppm	No of carbon atoms	<sup>13</sup> C chemical shift δ, ppm	No of carbon atoms	<sup>13</sup> C chemical shift δ, ppm
H56	0.76 (0.6298)	H60	3.47 (2.5547)	C8	15.23 (8.2091)	C3	127.70 (123.53)
H55	0.76 (0.713)	H32	3.08 (2.7222)	C20	22.22 (17.1025)	C36	126.50 (124.049)
H52	0.74 (0.850)	H23	3.08 (2.8077)	C50	25.32 (17.5175)	C10	127.80 (124.852)
H57	0.76 (0.8671)	H59	3.47 (2.8246)	C54	26.79 (19.4668)	C9	130.83 (130.394)
H65	1.36 (1.0295)	H29	3.08 (3.1171)	C47	39.59 (20.5518)	C11	139.73 (133.285)
H51	0.74 (1.0537)	H24	3.40 (3.5316)	C19	39.79 (22.1292)	C34	140.93 (134.961)
H25	1.54 (1.5054)	H64	4.98 (5.31)	C21	40 (23.8497)	C33	151.96 (148.554)
H27	1.68 (1.5312)	H58	5.41 (5.5037)	C13	40.21 (36.4849)	C4	157.06 (149.681)
H53	0.74 (1.5416)	H44	6.89 (6.1055)	C45	40.42 (39.5139)	C2	169.53 (170.732)
H30	1.68 (1.6262)	H38	7.13 (7.5597)	C22	54.42 (50.7651)	C14	172.54 (171.673)
H66	1.36 (1.7313)	H42	6.77 (7.5906)	C43	54.69 (51.4816)		
H49	1.54 (1.8271)	H41	7.03 (7.6747)	C18	54.42 (55.1463)		
H46	1.48 (1.8783)	H62	7.15 (7.7816)	C7	54.97 (74.4972)		
H48	1.59 (1.9064)	H40	7.30 (7.9629)	C35	64.56 (118.001)		
H67	1.36 (2.0015)	H61	6.89 (7.9849)	C12	114.83 (119.756)		
H26	1.68 (2.23)	H63	7.49 (8.4026)	C39	120.92 (119.786)		
H31	1.68 (2.2973)	H68	3.98 (3.7775)	C37	124.43 (121.944)		
H28	3.08 (2.4236)						

Found: experimental; (calc.): calculated by DFT.

obtained value of the parameter β (0.24) indicates a moderate covalent character for the metal—ligand bond. The magnetic susceptibility measurement value for the iron complex is 5.83 μB. The electronic spectrum of the copper(II) complex displays a band at 13550 cm<sup>-1</sup> which is assignable to the <sup>2</sup>B<sub>1g</sub>→<sup>2</sup>B<sub>2g</sub> transition. [22]. Its magnetic moment value of 1.88 μB, is characteristic of an octahedral configuration around the copper(II) atom. The Zn(II) complex showed an absorption band in the region of 32154 cm<sup>-1</sup> due to the ligand—metal charge transfer, which corresponds to all paired electrons [23]. This complex is diamagnetic and is likely to be octahedral.

Theoretical wavelengths (λ) are also calculated using the DFT method at the B3LYP/LanL2DZ level and are in reasonable agreement with the experimental results of the UV-Vis spectral data.

**Molecular modeling.** Geometry optimization. To obtain the molecular conformation of the complexes, energy minimization studies were carried out using DFT calculations.

Repaglinide ligand. The structural parameters of the optimized geometry of the repaglinide ligand are obtained from DFT-B3LYP calculations. The calculated parameters are informative and the data are drawn to give the optimized geometry of the molecule (Fig. 4).

The O1—C2 bond distance is 1.390 Å and the O1—C2—C3 bond angle (115.6°) reflects the *sp*<sup>2</sup> hybridization of C2. The O1—C2—C3—C4 dihedral angle (4.7°) indicates that O1 and C4 occupy the *cis* configuration. The value of 177.2° of the O6—C2—C3—C4 dihedral angle is evidence that the four atoms are not in the same plane. Fig. 5 shows the contour plots of the selected molecular orbitals of repaglinide. The highest occupied molecular orbital (HOMO) density is distributed over the piperidinophenyl group, N16, H58, and O15 atoms, while HOMO-1 covers benzoic acid and the ethoxy group. The lowest unoccupied molecular orbital (LUMO) level is localized over benzoic acid, the C13 and O15 atoms and LUMO+1 covers the phenyl group.

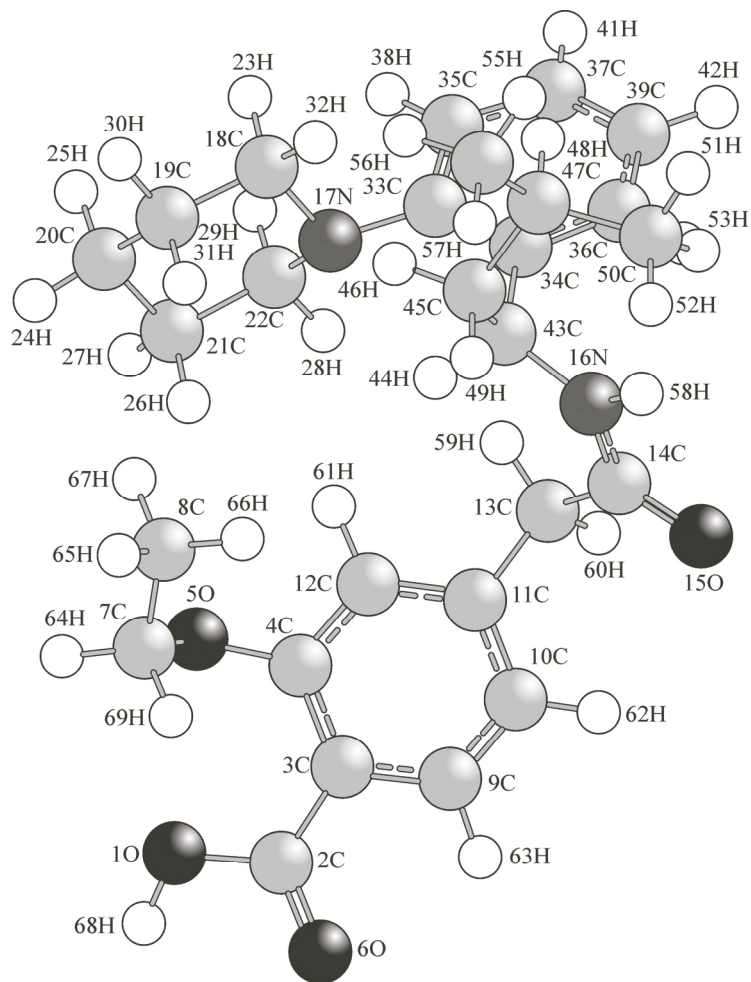


*Fig. 4.* Molecular structure of the HL ligand

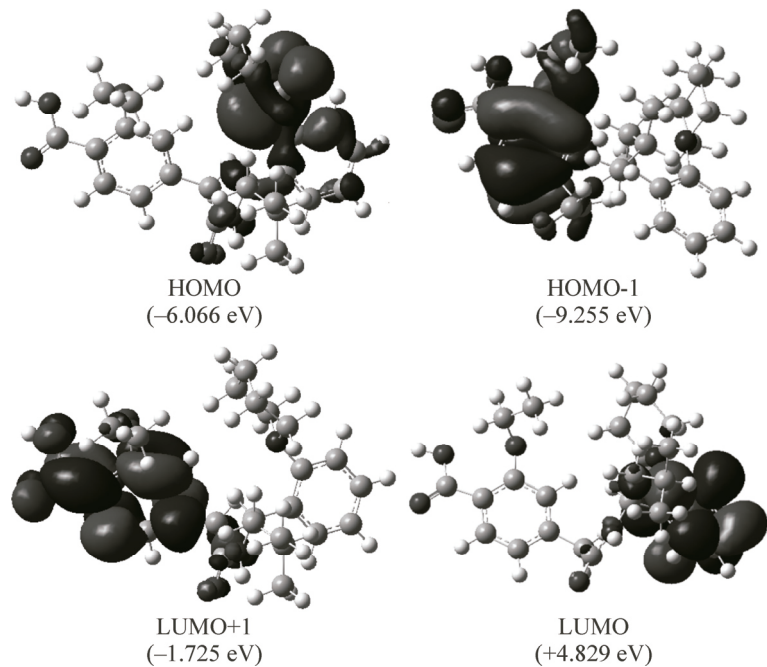


*Fig. 5.* Contour plots of some selected molecular orbitals of the repaglinide ligand

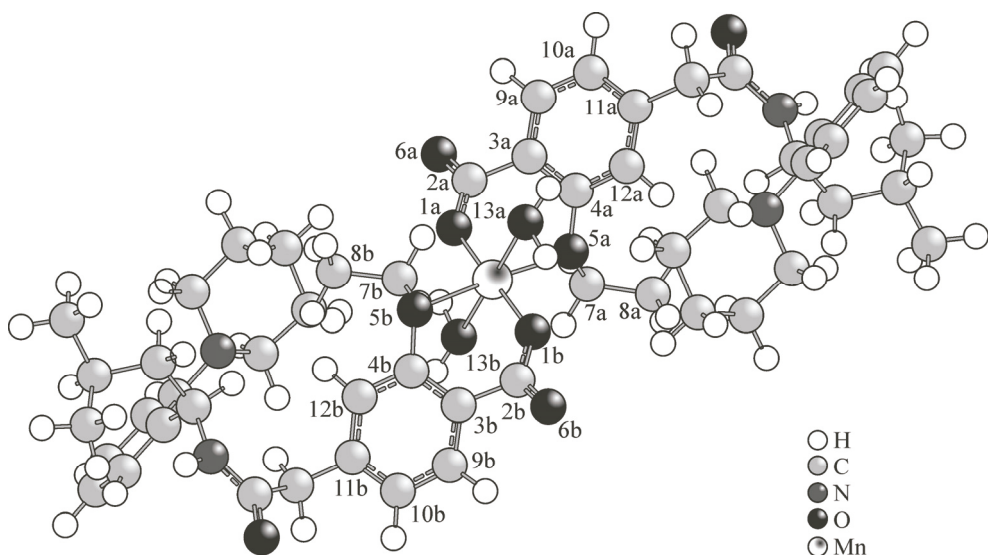


Fig. 6. Octahedral form of the Mn(II) complex

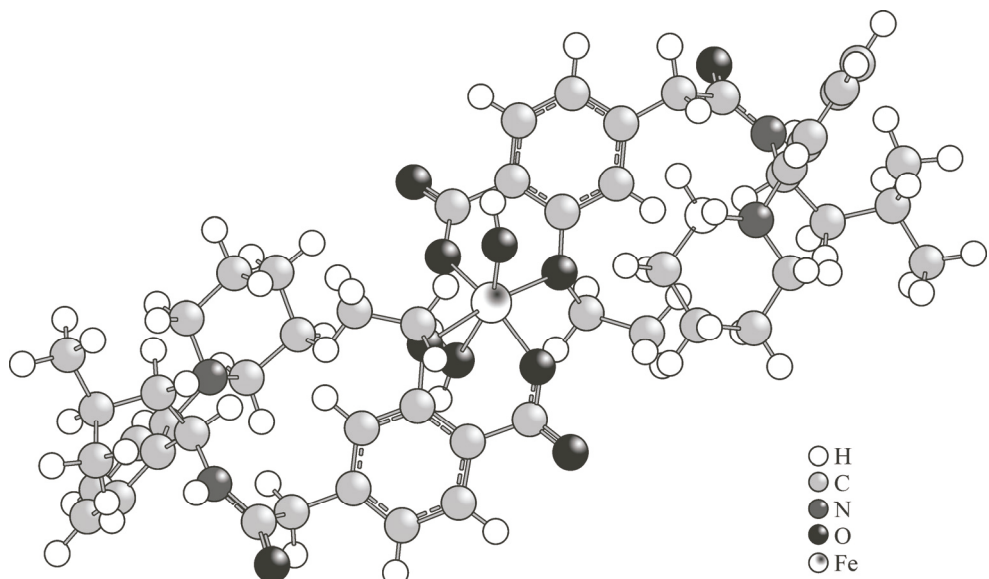


Fig. 7. Octahedral form of the Fe(III) complex

**Repaglinide complexes.** Bond length and bond angle calculations. The geometry has been optimized in the octahedral form for all the synthesized complexes. Each geometry optimization was completed by a calculation of harmonic vibrational frequencies to confirm the most stable geometry. Selected bond distances, bond angles, and dihedral angles for the manganese(II), iron(III), copper(II), and zinc(II) complexes (Figs. 6, 7) are listed in Table 3. When the bond lengths in the synthesized complexes are compared with those in the free repaglinide ligand, it is seen that coordination elongates the O5a—C7a bond from 1.481 to 1.500—1.507 Å for the synthesized complexes and contracts the O1a—C2a bond from 1.390 to 1.334—1.345 Å. These changes in bond lengths are attributable to the stabilization of the synthesized complexes upon complexation via loss of the COOH proton.

In the ML complexes ( $M = \text{Fe(III)}$  and  $\text{Cu(II)}$ ), the  $M—\text{O}1\text{a}$  bond lengths are 2.016 and 1.937 Å respectively. They are shorter than  $\text{Zn—O}1\text{a}$  and  $\text{Mn—O}1\text{a}$  bond lengths of 2.024 and 2.076 Å. The  $\text{Fe—O}1\text{a}$  bond length is longer than  $\text{Fe—O}1\text{b}$  by 0.086 Å. Also, it is found that the  $\text{Mn—O}5\text{b}$  and  $\text{Fe—O}5\text{b}$  bond lengths of 2.260 and 2.191 Å are longer than  $\text{Mn—O}5\text{a}$  and  $\text{Fe—O}5\text{a}$  bond lengths of

Table 3

Calculated structural parameters of the synthesized complexes

Parameters	Mn(II) complex	Fe(III) complex	Cu(II) complex	Zn(II) complex	Parameters	Mn(II) complex	Fe(III) complex	Cu(II) complex	Zn(II) complex
Bond length, Å					Bond angles, deg.				
M—O1a	2.076	2.016	1.937	2.024	O1a—M—O1b	179.1	156.1	179.6	178.8
M—O1b	2.076	1.930	1.937	2.023	O5a—M—O5b	178.5	171.8	178.9	178.2
M—O5a	2.255	2.122	2.113	2.184	O13a—M—O13b	179.8	164.2	179.9	179.7
M—O5b	2.260	2.191	2.126	2.187	O5a—M—O1a	79.8	81.9	85.5	82.2
M—O13a	2.254	1.845	2.354	2.180	O5b—M—O1b	79.5	82.6	85.0	81.8
M—O13b	2.261	2.256	2.350	2.190	O5a—M—O1b	101.4	101.9	94.1	96.8
O1a—C2a	1.335	1.345	1.342	1.334	O5b—M—O1a	99.4	90.9	95.4	99.3
O1b—C2b	1.334	1.340	1.340	1.332	O5a—M—O13a	86.6	95.1	85.8	86.4
O5a—C4a	1.428	1.424	1.425	1.427	O5b—M—O13b	86.0	83.5	85.5	85.9
O5b—C4b	1.429	1.428	1.427	1.429	O5b—M—O13a	93.5	91.7	94.4	94.2
O5a—C7a	1.500	1.507	1.504	1.500	O5a—M—O13b	93.5	91.2	94.1	93.5
O5b—C7b	1.500	1.513	1.505	1.500					
Dihedral angles, deg.									
O1a—M—O5a—C4a	56.1	53.8	54.6	55.2	C2b—C3b—C4b—O5b	4.6	7.1	3.7	4.8
O1b—M—O5b—C4b	56.0	47.9	55.1	55.3	C3a—C4a—O5a—C7a	88.6	106.8	91.2	92.1
M—O1a—C2a—C3a	1.1	5.0	2.0	1.2	C3b—C4b—O5b—C7b	86.7	93.7	88.0	90.2
M—O1b—C2b—C3b	0.3	9.1	4.9	0.3	C4a—O5a—C7a—C8a	83.4	98.0	81.4	81.5
O1a—C2a—C3a—C4a	28.6	21.3	24.8	27.3	C4b—O5b—C7b—C8b	82.2	89.2	78.0	82.5
O1b—C2b—C3b—C4b	28.1	25.7	23.5	26.7	C9a—C3a—C4a—C12a	3.8	4.1	3.8	4.1
C2a—C3a—C4a—O5a	4.3	4.4	3.5	4.5	C9b—C3b—C4b—C12b	3.7	4.0	3.6	3.9

2.255 and 2.122 Å, while the Cu—O13b bond length is shorter than Cu—O13a by 0.004 Å. These results indicate that the coordination geometry around the metal center is a distorted octahedron. [24, 25]. The O1a—M—O1b and O5a—M—O5b bond angles deviate from linearity (180°) for the complexes, indicating a distortion in the basal plane around these metal ions. The calculated M—O1a—C2a—C3a and M—O1b—C2b—C3b dihedral angles of 0.3—9.1 Å show a *cis* configuration of both metal—C3a and metal—C3b. Mn(II), Fe(III) Cu(II), and Zn(II) complexes are stable in the octahedral environment.

**Molecular parameters.** The molecular parameters: total energy, dipole moment, Mulliken charge, HOMO, LUMO, and energy gap were calculated and presented in Table 4. The minimized energies of Mn(II), Fe(III), Cu(II), and Zn(II) octahedral complexes decrease in the following order: Zn(II) complex > Mn(II) complex > Fe(III) complex > Cu(II) complex.

The dipole moment is the indicator of the symmetry of the molecules. The Fe(III) complex having the dipole moment value of 3.0 D is the lowest symmetrical complex compared to the other complexes.

The Mulliken charge is related to the electron density and is a very useful descriptor in understanding sites for the electrophilic attack and the nucleophilic reaction. The manganese, copper, and zinc valence in their complexes is 2+ and 3+ for complexed iron while the net charges of these metals are +0.787 e, +0.834 e, and +1.046 e, respectively for Mn(II), Fe(III), and Zn(II). The net charge of copper is lowest (+0.473 e), showing that the metal center in the studied complexes obtained part of electrons from ligand donor atoms. These results show that the covalent character of metal-ligand bonds decreases in the following order: Cu(II) complex > Mn(II) complex > Fe(III) complex > Zn(II) complex. The net charges of donor atoms (Table 4), confirm the electron transfer to metal ions.

Table 4

*Some energy properties of the synthesized complexes*

Parameters	Mn(II) complex	Fe(III) complex	Cu(II) complex	Zn(II) complex
Energy, a.u.	-3177.2632	-3196.1186	-3269.3990	-3138.8974
Dipole moment, Debye	0.4	3.0	1.0	0.7
Charge of Mulliken, e:				
M	0.787	0.834	0.473	1.046
O1a	-0.555	-0.529	-0.501	-0.589
O1b	-0.553	-0.473	-0.502	-0.586
O5a	-0.461	-0.476	-0.437	-0.484
O5b	-0.460	-0.459	-0.434	-0.484
O13a	-0.748	-0.701	-0.716	-0.771
O13b	-0.747	-0.721	-0.716	-0.770
HOMO, eV	-5.938	-5.853	-6.024	-6.019
LUMO, eV	-1.294	-3.514	-3.512	-1.315
$\Delta E$ , eV	4.644	2.339	2.512	4.704

The frontier orbitals HOMO and LUMO are very important parameters for the chemical reaction and take part in chemical stability [ 26—28 ]. The transitions can be described from HOMO to LUMO which determine the molecular electron transport properties. Fig. 8 shows the energy levels of HOMO and LUMO for the iron(III) complex.

For the manganese complex, the HOMO density is distributed over the metal, coordination water,  $\text{COO}^-$ , and the ethoxy group while the LUMO density covers the ethoxy and benzoic acid groups.

For iron, copper, and zinc complexes, HOMO is localized on the piperidinophenyl group.

The LUMO density covers iron,  $\text{H}_2\text{O}$ , and OH for the iron complex; copper,  $\text{COO}^-$ ,  $\text{H}_2\text{O}$ , and the ethoxy group for the copper complex, and benzoic acid for the zinc complex.

Higher HOMO energy values show that the molecule is a good electron donor and LUMO presents the ability of a molecule for receiving electrons.

Binding energies and stability. The complexation energy or binding energy  $E_{\text{complexation}}$  is estimated by the energy difference between the optimized complex  $E_{\text{complex}}$  and the single point energy of

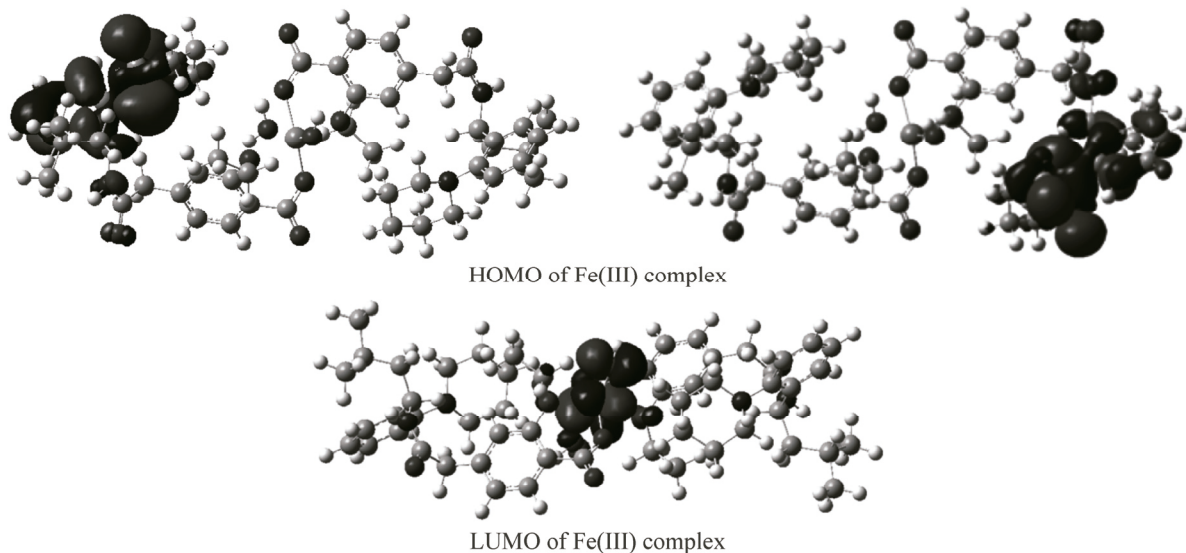


Fig. 8. Frontier molecular orbitals HOMO and LUMO of the iron(III) complex

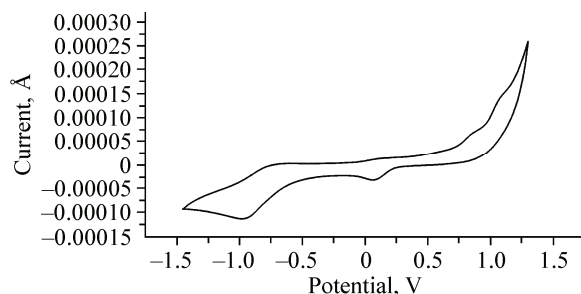


Fig. 9. Cyclic voltammogram of the copper(II) complex in 0.1 M TBAPF<sub>6</sub> in DMSO at 100 mV/s under N<sub>2</sub>

isolated metal  $E_{\text{metal}}$  (metal = Cu(II), Mn(II), Fe(III), and Zn(II)) and linking metal groups (L = anion ligand, H<sub>2</sub>O, and/or OH<sup>-</sup>) in the optimized complex, in the gas phase [29, 30]. The calculation of binding energies for various coordination complexes is performed as follows:

$$E_{\text{complexation}} = E_{\text{complex}} - (E_{\text{metal}} + \sum E_L).$$

The most stable complex corresponds to the greatest negative value of the complexation energy.

Table 5 presents the complexation energies for the studied complexes. As can be observed, the order of complexation energies for the obtained structures is as follows: Fe(III) complex < Cu(II) complex < Zn(II) complex < Mn(II) complex.

**Electrochemical behavior.** Cyclic voltammetry was carried out on a 10<sup>3</sup> M solution of the compounds in DMSO, containing 0.1 M tetrabutylammonium hexafluorophosphate (TBAPF<sub>6</sub>) as supporting electrolyte. The redox properties of the repaglinide ligand and Mn(II), Fe(III), Cu(II), and Zn(II) complexes have been studied in the DMSO solution at a platinum electrode, within a potential range from 1.5 to -1.5 V. The potentials were measured versus the saturated calomel electrode.

The cyclic voltammetry study of the complexes shows irreversible redox processes for all products. The frontier orbital LUMO for the repaglinide ligand is distributed over benzoic acid. This is proved by the appearance of a reduction wave at  $E_{pc} = -0.57$  V and an oxidation peak at -0.26 V in the ligand voltammogram. The obtained reduction in the voltammogram of Mn(II)L may be attributed to the Mn(II)/Mn(I) system at  $E_{pc} = -1.04$  V and  $E_{pa} = -0.71$  V. For the iron complex, LUMO is distributed over the metal center, which leads to an easier reduction for metal, therefore its voltammogram presents a first electrochemical process Fe(III)/Fe(II) at  $E_{pc} = -0.73$  V and  $E_{pa} = 0.45$  V. and a second process at  $E_{pc} = -0.91$  V and  $E_{pa} = -0.70$  V corresponding to the reduction of the ligand coordinated to the metal atom.

For the copper complex, LUMOs are distributed near the metal center allowing its easy reduction when it is coordinated to the repaglinide ligand. The copper complex has a cathodic peak at  $E_{pc} = -0.95$  V and an anodic one at  $E_{pa} = -0.75$  V, corresponding to Cu(I)/Cu(0) reduction (Fig. 9). The second reduction Cu(II)/Cu(I) appears at  $E_{pc} = 0.07$  V with  $E_{pa} = 0.84$  V. The oxidation peak at 1.06 V is due to the oxidation of Cu(II) to Cu(III) in the copper complex [31].

The comparison of the redox data of the repaglinide ligand and the zinc complex implies that the first reduction process corresponds to the repaglinide ligand,  $E_{pc} = -0.26$  V and  $E_{pa} = -0.024$  V. The second reduction process is attributed to the metal center reduction Zn(II)/Zn(I), which is observed at  $E_{pc} = -0.60$  V.

The presence of the repaglinide ligand in the complexes shifts the reduction potentials of the metal ions towards more negative values. It could be concluded that the complexation of metals stabilizes degree (II) for manganese, copper and zinc, and degree (III) for iron.

Table 5

Complexation energies (Kcal/mol) for the studied complexes obtained at the DFT level

Complex	$E_{\text{complexation}}$ , Kcal/mol
Mn(II) complex	-645.57
Fe(III) complex	-1440.22
Cu(II) complex	-715.87
Zn(II) complex	-673.98

## CONCLUSIONS

In the present study we have synthesized novel manganese(II), iron(III), copper(II), and zinc(II) complexes of repaglinide, which were characterized by several spectrometric methods. Spectral cha-

racterizations show that the coordination number of Mn(II), Fe(III), Cu(II), and Zn(II) ions is six and they have a distorted octahedral geometry. The comparison between the experimental and theoretical results indicates that the B3LYP/LANL2DZ density functional method is able to provide satisfactory results to predict the structural parameters.

The experimental FT-IR, UV-Visible spectra for all the complexes and  $^1\text{H}$  and  $^{13}\text{C}$  NMR for Zn(II)L are in reasonable correlation with the theoretical data (DFT).

The stability sequence observed for the studied complexes is: Fe(III) > Cu(II) > Zn(II) > Mn(II).

The HOMO-LUMO energy gap suggests the eventual charge transfer interactions taking place within the synthesized complexes. The redox behavior was explored by cyclic voltammetry based on the metal-centered reduction for all complexes. The reduction/oxidation potential depends on the structure and conformation of the central atom in the coordination compounds. The repaglinide ligand stabilise its complexes in the distorted octahedral geometry around the metal center.

Sihem Sadaoui-Kacel thanks the Algerian Ministry of Education and Research for providing a fellowship for a short stay in the Université de Rennes1, France. We thank Dr. Lahcène Ouahab and his colleagues from the Université de Rennes1 for their assistance with the elemental, spectroscopic analyses and electrochemical measurements.

#### REFERENCES

1. Djebbar-Sid S., Benali-Baitich O., Deloume J.P. // Trans. Met. Chem. – 1998. – **23**. – P. 443 – 447.
2. Belaid S., Djebbar S., Benali-Baitich O., Khan M.A., Bouet G. // C. R. Chim. – 2007. – **10**. – P. 568 – 572.
3. Djebbar-Sid S., Benali-Baitich O., Deloume J.P. // J. Mol. Struct. – 2001. – **569**. – P. 121 – 128.
4. Bouchoucha A., Terbouche A., Zaouani M., Derridj F., Djebbar S. // J. Trace Elem. Med. Biol. – 2013. – **27**. – P. 191 – 202.
5. Jana M.S., Pramanik A.K., Sarkar D., Biswas S., Mondal T.K. // Polyhedron. – 2014. – **81**. – P. 66 – 73.
6. Kozlowski H., Janicka-Klos A., Brasun J., Gaggelli E., Valensin D., Valensin G. // Coord. Chem. Rev. – 2009. – **253**. – P. 2665 – 2685.
7. Nicolescu C., Arama C., Monsiu C.M. // Farmacia. – 2010. – **58**. – P. 78 – 88.
8. Becke A.D. // J. Chem. Phys. – 1993. – **98**. – P. 5648 – 5652.
9. Hay P.J., Wadt W.R. // J. Chem. Phys. – 1985. – **82**. – P. 270 – 284.
10. Frisch M.J., Trucks G.W., Schlegel H.B., Scuseria G.E., Robb M.A., Cheeseman J.R., Montgomery J.A., Vreven T., Kudin K.N., Burant J.C., Millam J.M., Iyengar S.S., Tomasi J., Barone V., Mennucci B., Cossi M., Scalmani G., Rega N., Petersson G.A., Nakatsuji H., Hada M., Ehara M., Toyota K., Fukuda R., Hasegawa J., Ishida M., Nakajima T., Honda Y., Kitao O., Nakai H., Klene M., Li X., Knox J.E., Hratchian H.P., Cross J.B., Adamo C., Jaramillo J., Gomperts R., Stratmann R.E., Yazyev O., Austin A.J., Cammi R., Pomelli C., Ochterski J.W., Ayala P.Y., Morokuma K., Voth G.A., Salvador P., Dannenberg J.J., Zakrzewski V.G., Dapprich S., Daniels A.D., Strain M.C., Farkas O., Malick D.K., Rabuck A.D., Raghavachari K., Foresman J.B., Ortiz J.V., Cui Q., Baboul A.G., Clifford S., Cioslowski J., Stefanov B.B., Liu G., Liashenko A., Piskorz P., Komaromi I., Martin R.L., Fox D.J., Keith T., Al-Laham M.A., Peng C.Y., Nanayakkara A., Challacombe M., Gill P.M.W., Johnson B., Chen W., Wong M.W., Gonzalez C., Pople J.A. // Gaussian 03, Revision A.1. – Pittsburgh PA: Gaussian, Inc., 2003.
11. Fresch A., Nielson A.B., Holder A.J. // GAUSSVIEW User Manual. – Pittsburgh: Gaussian, Inc., 2003.
12. Kratz F., Nuber B., Weib J., Keppler B.K. // Synth. Inorg. Met. Org. Chem. – 1991. – **21**. – P. 1601 – 1613.
13. Liu J.N., Wu B.W., Zhang B., Liu Y. // Turk. J. Chem. – 2006. – **30**. – P. 41 – 48.
14. Refat M.S., El-Deen I.M., Ibrahim H.K., El-Ghool S. // Spectrochim Acta A. – 2006. – **65**. – P. 1208 – 1220.
15. Geeta B., Shravankumar K., Muralidhar Reddy P., Ravikrishna E., Sarangapani M., Krishna Reddy K., Ravinder V. // Spectrochim Acta A. – 2010. – **77**. – P. 911 – 915.
16. Huber P.C., Reis G.P., Amstalden M.C.K., Lancellotti M., Almeida W.P. // Polyhedron. – 2013. – **57**. – P. 14 – 19.
17. Mounika K., Anupama B., Pragathi J., Gyanakumari C. // J. Sci. Res. – 2010. – **2**. – P. 513 – 524.
18. Bosnich B. // J. Am. Chem. Soc. – 1968. – **90**. – P. 627 – 632.
19. Mohan M., Kumar M. // Trans. Met. Chem. – 1985. – **10**. – P. 255 – 258.
20. Belaid S., Landreau A., Djebbar S., Benali-Baitich O., Bouet G., Bouchara J.P. // J. Inorg. Biochem. – 2008. – **102**. – P. 63 – 69.
21. Mohamed G.G., El-Gamel N.E.A. // Vib. Spectrosc. – 2004. – **36**. – P. 97 – 104.
22. Aljahdali M., Ahmed el-Sherif A. // Inorg. Chim. Acta. – 2013. – **407**. – P. 58 – 68.

23. *Devi J., Batra N.* // Spectrochim Acta. – 2015. – **135**. – P. 710 – 719.
24. *Bouchoucha A., Terbouche A., Bourouina A., Djebbar S.* // Inorg. Chim. Acta. – 2014. – **418**. – P. 187 – 197.
25. *Abu-Eittah R.H., Zordok W.A.* // J. Mol. Struct.: THEOCHEM. – 2010. – **951**. – P. 14 – 20.
26. (a) *Fukui K.* // Science. – 1982. – **218**. – P. 747 – 754; (b) *Kumar R., Obrai S., Mitra J.* // Spectrochim. Acta, Part A. – 2013. – **115**. – P. 244 – 249.
27. *Terbouche A., Ait-Ramdane-Terbouche C., Djebbar S., Gerniche D., Bagtache R., Bensiradj N.E.H., Saal A., Hauchard D.* // J. Mol. Struct. – 2014. – **1076**. – P. 501 – 511.
28. *Tidjani-Rahmouni N., Bensiradj N.E.H., Djebbar S., Benali-Baitich O.* // J. Mol. Struct. – 2014. – **1075**. – P. 254 – 263.
29. *Bensouilah N., Abdaoui M.* // C. R. Chim. – 2012. – **15**. – P. 1022 – 1036.
30. *Ghosh D., Bagchi S., Das A.K.* // Mol. Phys. – 2012. – **110**. – P. 37 – 48.
31. *Djebbar-Sid S., Benali-Baitich O., Deloume J.P.* // Polyhedron. – 1997. – **16**. – P. 2175 – 2182.